

SLAC-PUB-4878

May 1989

(E/T)

**LIMITS ON DOUBLY-CHARGED HIGGS
BOSONS AND LEPTON FLAVOR VIOLATION***

MORRIS L. SWARTZ

*Stanford Linear Accelerator Center,
Stanford University, Stanford, California 94309*

We consider the effect of a doubly-charged Higgs boson (Δ^{--}) on several processes. We find that the effective Hamiltonian that is normally used to interpret the results of muonium-antimuonium oscillation experiments also describes the t-channel exchange of a Δ^{--} . A limit on the existence of the Δ^{--} is extracted from the most recent muonium oscillation result. The effect of Δ^{--} exchange on high energy Bhabha scattering is discussed, and a limit is extracted from the published cross sections of several PEP and PETRA experiments. The case of a non-diagonal coupling of the Δ^{--} to the charged leptons (non-diagonal in lepton flavor) is considered. A limit is extracted from the result of the most recent search for the rare decay $\mu \rightarrow 3e$. Finally, a coupling-independent limit is extracted from a recent measurement of the process $e^+e^- \rightarrow 4$ leptons at PETRA.

Submitted to Physical Review D

* Work supported by the Department of Energy, contract DE-AC03-76SF00515.

1. INTRODUCTION

The origin of the apparent family structure of all known fermions is a complete mystery. It has been known¹ since the discovery of the kaon that the weak eigenstates of the quark sector do not respect this family structure. However, no analogous behavior has ever been observed in the lepton sector. Most searches for lepton flavor violation have concentrated upon processes which change lepton flavor, ΔL_f ,² by one unit (e.g., $K \rightarrow \mu e$ or $\mu \rightarrow e \gamma$). There have been relatively few searches done for those processes that change lepton flavor by two units.

The first searches for $\Delta L_f = 2$ transitions were motivated by the realization that the absence of the decay $\mu \rightarrow e \gamma$ could be explained by a multiplicative quantum number instead of an additive one.³ Feinberg and Weinberg⁴ suggested a number of experimental tests of this idea. Two of their suggestions were to search for the process $e^- e^- \rightarrow \mu^- \mu^-$, and to search for the transformation of muonium ($\mu^+ e^- \equiv M$) into antimuonium ($\mu^- e^+ \equiv \bar{M}$). This latter process is the exact analog of $K^0 - \bar{K}^0$ mixing. In the absence of external electromagnetic fields and assuming that the mass difference of the mixed states, δ , is small, the probability of observing a transition, $P(\bar{M})$, can be written as

$$P(\bar{M}) \simeq \frac{\delta^2}{2\Gamma_\mu^2} \quad , \quad (1)$$

where Γ_μ is the muon decay rate. Feinberg and Weinberg assumed that the transition could be characterized by an effective Hamiltonian of the form

$$\mathcal{H}_{M\bar{M}} = \frac{G_{M\bar{M}}}{\sqrt{2}} \bar{\psi}_\mu \gamma^\alpha (1 + \gamma_5) \psi_e \bar{\psi}_\mu \gamma_\alpha (1 + \gamma_5) \psi_e + \text{h.c.} \quad , \quad (2)$$

where $G_{M\bar{M}}$ is an effective four-fermion coupling constant. They then calculated that the mass difference for the hyperfine $J = 0$ and $J = 1$ states would be of the form

$$\delta \equiv 2 \cdot \langle \bar{M} | \mathcal{H}_{M\bar{M}} | M \rangle = \frac{16G_{M\bar{M}}}{\sqrt{2}\pi a^3} \quad , \quad (3)$$

where a is the Bohr radius ($a^{-1} = \alpha m_e$).

In the late 1960's, a group at the Los Alamos Meson Facility⁵ searched for the spontaneous conversion of muonium into antimuonium. They did not observe a signal and were able to place an upper limit⁶ on $G_{M\bar{M}}$ of $5800 \cdot G_F$, where G_F is the Fermi coupling constant. A second group working the Princeton-Stanford electron storage rings⁷ searched for the process $e^-e^- \rightarrow \mu^-\mu^-$. They also obtained a null result. Using Eq. (2) to calculate the expected cross section, they placed an upper limit on $G_{M\bar{M}}$ of $610 \cdot G_F$. Since that time, several groups have searched for muonium-antimuonium conversion.^{8,9} The most sensitive search to date⁹ has established an upper limit on $G_{M\bar{M}}$ of $1.1 \cdot G_F$.

It is interesting to note that none of these results rules out the presence of a multiplicative quantum number (which would presumably allow muonium-antimuonium conversion and double electron-muon conversion to proceed with a characteristic coupling $G_{M\bar{M}} \approx G_F$). The absence of a multiplicative lepton quantum number is inferred from the small size of the branching ratio of $\mu^+ \rightarrow e^+\bar{\nu}_e\nu_\mu$,¹⁰

$$\frac{\Gamma(\mu^+ \rightarrow e^+\bar{\nu}_e\nu_\mu)}{\Gamma(\mu^+ \rightarrow e^+\nu_e\bar{\nu}_\mu)} \leq 0.098 \quad ,$$

and from a measurement of the ratio of inverse muon decay cross sections,¹¹

$$\frac{\sigma(\bar{\nu}_\mu e^- \rightarrow \mu^-\bar{\nu}_e)}{\sigma(\nu_\mu e^- \rightarrow \mu^-\nu_e)} \leq 0.05 \quad .$$

In the years since the original work of Feinberg and Weinberg, a number of physical models have been proposed that incorporate lepton flavor changing processes. Feynman diagrams for three processes that mediate the conversion of muonium into antimuonium¹² are shown in Fig. 1.

Diagram (a) represents the second-order exchange of ordinary massive Dirac neutrinos. Since the external (lepton) masses are at least as large as the internal (neutrino) masses, this process is more analagous to $B^0-\bar{B}^0$ mixing than to neutral kaon mixing. Several authors¹³ have calculated the effective Hamiltonian for B meson mixing. Changing quark labels to lepton labels, we can write that the effective Hamiltonian for second-order neutrino exchange is given by the expression

$$\begin{aligned} \mathcal{H}_{\text{eff}} = & \frac{G_A}{\sqrt{2}} \bar{\psi}_\mu \gamma^\alpha (1 + \gamma_5) \psi_e \bar{\psi}_\mu \gamma_\alpha (1 + \gamma_5) \psi_e \\ & + \frac{G_B}{\sqrt{2}} \bar{\psi}_\mu (1 - \gamma_5) \psi_e \bar{\psi}_\mu (1 - \gamma_5) \psi_e + \text{h.c.} \quad , \end{aligned} \quad (4)$$

where the coupling constants G_A and G_B are complicated functions of lepton masses, neutrino masses, and mixing angles. Equation (4) differs from Eq. (2) by the inclusion of a second term. The effect of the second term on the mass difference is comparable in magnitude (but opposite in sign) to that of the first term. Using expressions given in Ref. 13, it is straightforward to estimate the following *very conservative* upper bound for G_A and G_B ,

$$G_A, G_B < \frac{G_F^2 \sqrt{2}}{8\pi^2} m_\mu^2 = 7 \times 10^{-9} \cdot G_F \quad .$$

This is more than eight orders of magnitude smaller than the best experimental limit on G_{MM} .

The process represented by diagram (b) is quite similar to that represented by diagram (a) except that Majorana neutrinos are exchanged instead of Dirac ones.

Halprin¹⁴ has noted that the absence of neutrinoless double-beta decay implies that this process must occur with an effective coupling $G_{MM} \lesssim 3 \times 10^{-5} \cdot G_F$. This is also well below the limit of observability.

The third process shown in Fig. 1, diagram (c) involves the t-channel exchange of a doubly-charged Higgs boson. A number of authors¹⁴⁻¹⁸ have considered the effect of doubly-charged Higgs bosons on various lepton number violating processes. Observable effects have not been ruled out by other processes.

2. DOUBLY-CHARGED HIGGS BOSONS

There is a large body of literature that deals with doubly-charged Higgs bosons of various types.^{17,19,20} Although they can arise in a number of scenarios, doubly-charged Higgs bosons are a natural feature of right-left symmetric models. Since they couple only to charged lepton pairs, other Higgs bosons, and gauge bosons, they contribute only to the higher-order corrections of processes that involve hadrons. Many of the most sensitive tests of lepton flavor conservation make use of initial state hadrons. The limits on the existence of doubly-charged Higgs bosons are therefore relatively weak.

In most models, the coupling of a doubly-charged Higgs boson, Δ^{--} , to a pair of leptons of flavor ℓ can be described by the following Lagrangian density:

$$\mathcal{L}_R = g_{\ell\ell} \Delta^{--} \bar{\psi}_{\ell R} \psi_{\ell}^c + (\text{h.c.}) \quad , \quad (5)$$

where: $g_{\ell\ell}$ is a dimensionless coupling constant; $\psi_{\ell R} = 1/2 (1 + \gamma_5) \psi_{\ell}$ is the right-handed charged lepton field; and $\psi_{\ell}^c = C \bar{\psi}_{\ell}^T$ is the charge conjugate field. In some models, the Δ^{--} couples to left-handed fields rather than the right-handed ones of Eq. (5). In the right-left symmetric models there are scalars, Δ_R and Δ_L , which

couple to right-handed and left-handed fermions, respectively. However, since most of the experimental processes that we shall consider are insensitive to the chirality of the lepton fields, we choose to consider only the right-handed case.²¹ It is worth noting that Eq. (5) describes the coupling of the doubly-charged Higgs scalar to a pair of right-handed leptons. Contrary to the claims of Ref. 16, this coupling is not helicity suppressed.

The mass of the doubly-charged Higgs boson, M_Δ , is certainly large on the scale of the momentum transfer that is associated with muonium to antimuonium oscillation. The effective hamiltonian for $M-\bar{M}$ conversion can therefore be written as

$$\mathcal{H}_\Delta = \frac{g_{ee}g_{\mu\mu}}{M_\Delta^2} \bar{\psi}_e^c \psi_{eR} \bar{\psi}_{\mu R} \psi_\mu^c + (\text{h.c.}) \quad . \quad (6)$$

It is instructive to transform Eq. (6) into a form more like Eq. (2). This can be done by first performing a Fierz transformation, and then by transposing the scalar (in Dirac space) formed from the product of the charge conjugate fields. The effective Hamiltonian can then be written as:

$$\mathcal{H}_\Delta = \frac{g_{ee}g_{\mu\mu}}{8M_\Delta^2} \bar{\psi}_\mu \gamma^\alpha (1 + \gamma_5) \psi_e \bar{\psi}_\mu \gamma_\alpha (1 + \gamma_5) \psi_e + (\text{h.c.}) \quad . \quad (7)$$

Equation (7) is identical to Eq. (2) with the coupling constant $G_{M\bar{M}}$ defined as

$$G_{M\bar{M}} \equiv \frac{g_{ee}g_{\mu\mu}}{4\sqrt{2}M_\Delta^2} = \frac{g_{ee}g_{\mu\mu}}{g^2} \left(\frac{M_w}{M_\Delta} \right)^2 \cdot G_F \quad , \quad (8)$$

where g is the SU(2) coupling constant and M_w is the W boson mass.

Using Eq. (8), the current limit⁹ on G_{MM} can be converted into a limit on the ratio of couplings to M_Δ^2 ,

$$\frac{g_{ee}g_{\mu\mu}}{M_\Delta^2} < 6.6 \times 10^{-5} \text{ GeV}^{-2} \quad (90\% \text{ CL}) .$$

This limit is represented graphically in Fig. 2 as a contour of M_Δ versus $\sqrt{g_{ee}g_{\mu\mu}}$. Note that some authors¹⁶ expect that the coupling constants $g_{\ell\ell}$ could be as large or larger than the electromagnetic coupling. To indicate the mass limits that correspond to such statements, the values of the coupling constants e , g' , and g are shown in the figure.

3. OTHER VIRTUAL PROCESSES

Those processes that exhibit explicit lepton flavor violation may be the most spectacular to contemplate but are not necessarily the most sensitive ones to use in experimental searches. In many cases, the most sensitive limits on new physical processes come from precision measurements of rather mundane processes.²² The following section describes a study of the rather mundane process of Bhabha scattering. We then consider the case in which the doubly-charged Higgs boson couples non-diagonally (in lepton flavor) to the charged lepton sector. In that case, very stringent limits can be obtained from the existing limit on the branching ratio for the process $\mu \rightarrow 3e$.

3.1. BHABHA SCATTERING

Doubly-charged Higgs scalars contribute to Bhabha scattering at the tree level. As is shown in Fig. 3, this involves the t-channel exchange of a Δ^{--} . If we assume

that M_Δ is large as compared with the center-of-mass energy of the scattering process, the effective Hamiltonian for this process can be written as

$$\mathcal{H}_{\text{Bhabha}} = \frac{g_{ee}^2}{M_\Delta^2} \bar{\psi}_e^c \psi_{eR} \bar{\psi}_{eR} \psi_e^c + (\text{h.c.}) \quad (9)$$

Equation (9) is identical to Eq. (6) except that the muon labels have been replaced by electron labels. Performing exactly the same mathematical transformations as were applied to Eq. (6), the Hamiltonian can be written as

$$\mathcal{H}_{\text{Bhabha}} = \frac{g_{ee}^2}{2M_\Delta^2} \bar{\psi}_{eR} \gamma^\alpha \psi_{eR} \bar{\psi}_{eR} \gamma_\alpha \psi_{eR} + (\text{h.c.}) \quad , \quad (10)$$

where we have chosen to express all fields as chiral fields.

The advantage of the form given by Eq. (10) is that it is very similar to one used by Eichten, Lane, and Peskin²³ to describe quark and lepton compositeness. In fact, Eq. (10) is identical to Eq. (1) of Ref. 23 if we choose the parameters of their model as follows: $\eta_{RR} = 1$; $\eta_{LL} = \eta_{RL} = 0$; $g = g_{ee}$; and $\Lambda = M_\Delta$. It is then trivial to extract the cross section for unpolarized Bhabha scattering from Eq. (2) of Ref. 23,

$$\sigma_{\text{Higgs}}(\cos \theta) \equiv \frac{d\sigma}{d(\cos \theta)} = \frac{\pi\alpha^2}{4s} \left[4A_0 + A_-(1 - \cos \theta)^2 + A_+(1 + \cos \theta)^2 \right] \quad , \quad (11)$$

where the coefficients A_0 , A_- , and A_+ are defined as

$$\begin{aligned} A_0 &= \left(\frac{s}{t} \right)^2 \left| 1 + \frac{g_r g_l}{e^2} \frac{t}{t_z} \right|^2 \\ A_- &= \left| 1 + \frac{g_r g_l}{e^2} \frac{s}{s_z} \right|^2 \\ A_+ &= \frac{1}{2} \left| 1 + \frac{s}{t} + \frac{g_r^2}{e^2} \left(\frac{s}{s_z} + \frac{s}{t_z} \right) + \frac{2g_{ee}^2 s}{e^2 M_\Delta^2} \right|^2 + \frac{1}{2} \left| 1 + \frac{s}{t} + \frac{g_l^2}{e^2} \left(\frac{s}{s_z} + \frac{s}{t_z} \right) \right|^2 \quad . \end{aligned}$$

The various quantities used in Eq. (11) are defined as follows: θ is the scattering angle in the cm frame; s is the square of the cm frame energy; $t = -s(1 - \cos \theta)/2$;

$s_z = s - M_z^2 + iM_z\Gamma_z$ (M_z and Γ_z are the mass and width of the Z^0 , respectively);
 $t_z = t - M_z^2 + iM_z\Gamma_z$; $g_r = e \tan \theta_w$ (e and θ_w are the electric charge and electroweak
 mixing angle, respectively); and $g_l = -e \cot 2\theta_w$.

Strictly speaking, Eq. (11) is valid only for the case $M_\Delta^2 \gg s$. If s is comparable
 to or larger than M_Δ^2 , the coefficient A_+ must be modified to account for the effect
 of the Δ^{--} propagator. The modification can be determined by performing the
 usual Fierz reordering and transposition of the charge conjugate current on the
 correct amplitudes (shown graphically in Fig. 3) rather than on the Hamiltonian.
 Comparing these amplitudes with those that are given by Eq. (10), we note that it is
 only necessary to replace M_Δ^2 by the expression $M_\Delta^2 - t'$ where $t' = -s(1 + \cos \theta)/2$.

Several e^+e^- experiments (TASSO,²⁴ PLUTO,²⁵ HRS,²⁶ and MAC²⁷) have
 searched for the contact terms described in Ref. 23. All of them have published
 95% confidence limits on the composite mass scale Λ for the $\eta_{RR} = 1$ case. These
 can easily be converted into limits on the ratio g_{ee}^2/M_Δ^2 in the *high mass* region.
 Unfortunately, they do not apply to the lower mass region, $M_\Delta \lesssim \sqrt{s}$, where the
 Higgs propagator effects are large. Fortunately, however, all of the above exper-
 iments have also published their measured cross sections. The following section
 discusses an analysis of their data to extract a single 90% confidence region in
 $g_{ee} - M_\Delta$ space.

Experimental Results

The parameters of the measurements of the Bhabha Scattering cross section by
 the two PEP experiments and the two PETRA experiments are given in Table I.

The data of the two PETRA experiments (PLUTO and TASSO) were presented
 in essentially identical formats. Both groups published the differential cross section

in an absolutely normalized form and in a form that was normalized to the expected QED cross section (including radiative corrections). The latter form can be defined as

$$R_{exp}(\cos \theta_i) \equiv \frac{\sigma_{exp}(\cos \theta_i)}{\sigma_{QED}(\cos \theta_i)} \quad , \quad (12)$$

where: $\cos \theta_i$ is a bin of scattering angle; σ_{exp} is the measured differential cross section; and σ_{QED} is the third-order QED differential cross section from a calculation of Berends and Kleiss.²⁸ The data of both groups were binned in exactly the same way: 19 bins from $\cos \theta = 0.8$ to $\cos \theta = -0.8$. The measurements of the HRS collaboration were presented as an absolutely normalized differential cross section of 22 bins from $\cos \theta = 0.55$ to $\cos \theta = -0.55$. There was sufficient information in their paper to convert their measurements into the form given by Eq. (12). The resolution of the MAC detector was not adequate to reliably identify the signs of final state electrons. Their results were therefore given in bins of the absolute value of the cosine of the scattering angle $|\cos \theta_i| \equiv \cos \theta_i + \cos(-\theta_i)$. Their measurements were presented as an absolutely normalized cross section in nine bins from $|\cos \theta| = 0.0$ to $|\cos \theta| = 0.9$. As in the case of the HRS measurements, it was straightforward to convert the MAC measurements into the form given by Eq. (12).

For each of the above measurements, the point-to-point systematic uncertainties were added in quadrature with the statistical error of each data point. In all cases, the statistical error was the dominant component of the total error. The overall normalizations of the four measurements were determined by four different procedures. Each group quotes a normalization uncertainty in the range 1% \rightarrow 3%.

It is assumed in the following analysis that the size of the radiative corrections that affect the weak neutral current and Higgs exchange processes are much smaller

than those associated with the underlying QED process.²⁹ In this approximation, the measured ratios that are defined in Eq. (12) can be compared directly with the quantity R_{tree} ,

$$R_{tree}(\cos\theta) \equiv \frac{\sigma_{Higgs}(\cos\theta)}{\sigma_{QED}^{\circ}(\cos\theta)} \quad , \quad (13)$$

where σ_{Higgs} is defined by Eq. (11) and where σ_{QED}° is the tree level QED cross section. Note that σ_{QED}° is trivially derived from Eq. (11) by setting $g_r = g_l = g_{ee} = 0$.

The data were analyzed by performing a simultaneous χ^2 fit of R_{tree} to the 69 measurements of R_{exp} from the four experiments. The overall normalizations of the four samples were allowed to vary as free parameters in all fits. The analysis was performed in three steps to insure that the procedure is self-consistent.

The data were first fit to the form of R_{tree} that includes QED effects only,

$$R_{tree} = C_i \quad , \quad (14)$$

where C_i is the normalization of the i^{th} sample ($i = 1, 4$). The minimum value of χ^2 was 76.8 for 65 degrees of freedom. This corresponds to a chisquare probability of 0.15.

The data were then fit to the form of R_{tree} that includes all electroweak effects. This form is given by Eqs. (13) and (11) with the coupling constant g_{ee} constrained to zero. The four normalizations and $\sin^2\theta_w$ were allowed to vary as free parameters. Note that both M_z and Γ_z were correctly scaled to $\sin^2\theta_w$. The minimum value of χ^2 was 58.3 for 64 degrees of freedom. The chisquare probability was improved to 0.81 by the inclusion of the weak corrections. The best estimate of $\sin^2\theta_w$ was $0.273_{-0.097}^{+0.073}$ which is consistent with the world average³⁰ of 0.230.

Finally, the Higgs exchange term was included in the definition of R_{tree} (the propagator corrected version of Eq. (11) was used). A series of fits were performed with the value of $\sin^2\theta_w$ constrained to 0.230, and with the mass M_Δ constrained to a number of values from 10 GeV to 2 TeV. The four normalizations and the coupling constant g_{ee}^2 were allowed to vary as free parameters. As one would expect, the best estimate of g_{ee}^2 scaled as g_{ee}^2/M_Δ^2 in the high mass region. In this region, the minimum value of χ^2 was 58.3 for 64 degrees of freedom. The best estimate of g_{ee}^2/M_Δ^2 was $(1.9 \pm 4.8) \times 10^{-6} \text{ GeV}^{-2}$. The following confidence intervals were obtained:

$$\begin{aligned} \frac{g_{ee}^2}{M_\Delta^2} &< 8.0 \times 10^{-6} \text{ GeV}^{-2} \quad (90\% \text{ CL}) \\ \frac{g_{ee}^2}{M_\Delta^2} &< 9.7 \times 10^{-6} \text{ GeV}^{-2} \quad (95\% \text{ CL}) \end{aligned}$$

In the low mass region ($M_\Delta < 50 \text{ GeV}$), the fit quality remained quite good (at $M_\Delta = 10 \text{ GeV}$, the value of χ^2 was 58.5). The effect of the Higgs propagator was to produce a less restrictive limit on g_{ee} in this region. The limit is summarized in Fig. 2 as a contour in $g_{ee} - M_\Delta$ space. For the case $g_{ee} = g_{\mu\mu}$, this limit is nearly three times more stringent than the one derived from the muonium-antimuonium limit.

To insure that this result is not sensitive to our choice of $\sin^2\theta_w$, the data were fit to R_{tree} with both $\sin^2\theta_w$ and g_{ee}^2 allowed to vary. A result that is very similar to the one shown in Fig. 2 was obtained.

We note that the cross section as described by Eq. (11) is not right-left symmetric. The term corresponding to exchange of the right-handed Higgs boson interferes with the right-handed part of the weak neutral current. A left-handed Higgs boson would interfere with the left-handed part of the weak neutral current.

Since right- and left-handed electrons couple with different strengths to the Z^0 , a left-handed Higgs boson would not produce exactly the same effect on the cross section. However, since the size of the $\Delta^{--} - Z^0$ interference term is quite small at PEP and PETRA energies, the limits shown in Fig. 2 apply equally well to the left-handed case.

In order to check the results given in Fig. 2, the measurements of each experiment were analyzed individually. Each group used somewhat different assumptions to derive their published limits for the composite mass scale Λ ($\Lambda = M_\Delta$ in the case $g_{ee} = \sqrt{4\pi}$). We were able to duplicate the results of three of the four experiments.

3.2. MUON DECAY

Many of the best limits on lepton flavor violation come from searches for rare decay modes of the muon.³¹ If the coupling of the doubly-charged higgs boson to the charged lepton is purely diagonal in the lepton flavor [as described in Eq. (5)], the Δ^{--} does not mediate muon decay at tree level. However, if (as several authors have suggested^{20,17}) the Δ^{--} does have non-diagonal couplings to leptons, it can mediate the decay $\mu^- \rightarrow e^- e^+ e^-$. This process is shown diagrammatically in Fig. 4. The non-diagonal coupling can be defined by the following Lagrangian:

$$\mathcal{L}_{e\mu} = g_{e\mu} \Delta^{--} \bar{\psi}_{eR} \psi_\mu^c + (\text{h.c.}) \quad , \quad (15)$$

where the coupling constant $g_{e\mu}$ is presumably suppressed by the sine of a mixing angle as compared with the diagonal coupling constants.

Using Eq. (15) it is straightforward to express the effective Hamiltonian for the decay $\mu^- \rightarrow e^- e^+ e^-$ as

$$\begin{aligned} \mathcal{H}_{\mu \rightarrow 3e} &= \frac{g_{e\mu} g_{ee}}{M_\Delta^2} \bar{\psi}_e^c \psi_{\mu R} \bar{\psi}_{eR} \psi_e^c + (\text{h.c.}) \\ &= \frac{g_{e\mu} g_{ee}}{8M_\Delta^2} \bar{\psi}_e \gamma^\alpha (1 + \gamma_5) \psi_e \bar{\psi}_e \gamma_\alpha (1 + \gamma_5) \psi_\mu + (\text{h.c.}) \quad , \end{aligned} \quad (16)$$

where we have made the usual transformations. Using Eq. (16) to calculate the $\mu \rightarrow 3e$ branching ratio, we find that

$$Br(\mu \rightarrow 3e) \equiv \frac{\Gamma(\mu^- \rightarrow e^- e^+ e^-)}{\Gamma(\mu^- \rightarrow e^- \nu_\mu \bar{\nu}_e)} = \frac{g_{e\mu}^2 g_{ee}^2}{16G_F^2 M_\Delta^4} = 2 \cdot \left(\frac{g_{e\mu} g_{ee}}{g^2} \right)^2 \left(\frac{M_w}{M_\Delta} \right)^4 \quad . \quad (17)$$

The best published limit³² on the branching ratio of $\mu \rightarrow 3e$ is $Br(\mu \rightarrow 3e) < 1.0 \times 10^{-12}$ at 90% confidence. Using Eq. (17), we find that the limit on $g_{e\mu} g_{ee} / M_\Delta^2$ is

$$\frac{g_{e\mu} g_{ee}}{M_\Delta^2} < 4.7 \times 10^{-11} \text{ GeV}^{-2} \quad (90\% \text{ CL}) \quad .$$

This very impressive limit does not readily fit on the scale of Fig. 2. It is sufficient to say that if the relevant mixing angle, $\theta_{e\mu}$, is larger than 6×10^{-6} , this limit is the most stringent one on the existence of doubly-charged Higgs bosons.

4. THE SEARCH FOR REAL Δ^{--}

The limits on the existence of doubly-charged Higgs bosons that are obtained from the study of virtual processes have the property that the limit on the mass M_Δ is correlated with the size of the coupling $g_{\ell\ell}$. This correlation can be removed

by searching for the production of real $\Delta^{--}\Delta^{++}$ pairs. The process $e^+e^- \rightarrow \Delta^{--}\Delta^{++}$ would produce rather spectacular four-lepton events (such as $e^-e^-\mu^+\mu^+$ combinations). While it is likely that such events would have been observed if a low-mass, doubly-charged Higgs boson did exist, there are no published searches for them. There are, however, several studies of ordinary four-lepton production available in the literature. The following section describes the extraction of a coupling-independent limit from published measurements of the process $e^+e^- \rightarrow 4$ leptons.

4.1. THE CROSS SECTION FOR $e^+e^- \rightarrow \Delta^{--}\Delta^{++}$

The tree-level differential cross section for the process $e^+e^- \rightarrow \Delta^{--}\Delta^{++}$ is given by the following expression,

$$\frac{d\sigma}{d(\cos\theta^*)} = \frac{\pi\alpha^2 Q_\Delta^2}{4s} (1 - \cos^2\theta^*) \left[1 - \frac{4M_\Delta^2}{s}\right]^{3/2}, \quad (18)$$

where \sqrt{s} is the total center-of-mass frame energy of the e^+e^- system; θ^* is the polar angle of the outgoing Δ^{--} with respect to the incident electron direction; and Q_Δ is the charge of the Higgs boson ($Q_\Delta = 2$). The total cross section for the process can therefore be written as

$$\sigma = \frac{4\pi\alpha^2}{3s} \left[1 - \frac{4M_\Delta^2}{s}\right]^{3/2}. \quad (19)$$

In the limit $M_\Delta^2/s \rightarrow 0$, the total cross section is equal to the cross section for the production of muon pairs (or in the language of electron-positron physics, the cross section is equal to one unit of R).

Each of the Higgs bosons then decays into a same-sign pair of leptons with a characteristic rate $\Gamma_{\ell\ell}$ that is given by the following expression,

$$\Gamma_{\ell\ell} = \frac{g_{\ell\ell}^2}{8\pi} M_{\Delta} \left[1 - \frac{2m_{\ell}^2}{M_{\Delta}^2} \right] \left[1 - \frac{4m_{\ell}^2}{M_{\Delta}^2} \right]^{1/2}, \quad (20)$$

where m_{ℓ} is the lepton mass. The Higgs bosons are therefore short-lived (in an experimental sense) unless the coupling constants $g_{\ell\ell}$ are *very small* (less than 10^{-9}).

4.2. EXPERIMENTAL RESULTS

A number of groups have studied the process $e^+e^- \rightarrow e^+e^-\ell^+\ell^-$ at PEP and PETRA energies. In most cases, they did not require that both of the electrons were observed. Only two groups have published data on large-angle, doubly-tagged events.³³⁻³⁵

The most complete and useful of these publications is the thesis by F. Le Diberder,³⁵ which describes an analysis of the data of the CELLO collaboration. His analysis is based upon a data sample that was taken at nine different beam energies from 17.5 GeV to 23 GeV. The sample corresponds to an integrated luminosity of 137 pb^{-1} . Part of the analysis was a search for final states with four large-angle (polar angle larger than 23°) electrons and/or muons. He observed a total of 25 four-lepton events in three distinct final states. The observed number of events is in excellent agreement with that expected from a Monte Carlo calculation of Berends, Daverveldt, and Kleiss.³⁶ A summary of these observations is given in Table II. The background from various other processes (tau pair production and leakage from other two-photon final states) was estimated to be small (roughly one event in the four-electron mode).

Simulation of the Doubly-Charged Higgs Process

In order to estimate the number of events that would have been observed if doubly-charged Higgs bosons were produced, we have performed a Monte Carlo simulation of the process $e^+e^- \rightarrow \Delta^{--}\Delta^{++} \rightarrow 4$ leptons for the CELLO detector. The simulation is based upon the cross section as given by Eq. (18). Since the threshold behavior of the cross section near the kinematic limit is quite important, we have included the effect of initial state bremsstrahlung by using the structure function approach of Nicosini and Trentadue.³⁷ Each Higgs boson was allowed to decay isotropically into lepton pairs. In order to study the leakage of tau decays into the electron and muon channels, the three lepton flavors were simulated according to a hypothetical set of branching ratios. The tau simulation included all spin correlations for the dominant single prong decay modes (spin correlations were not included for the nonresonant decays $\tau^\pm \rightarrow \pi^\pm + N\pi^0 + \nu$, N an integer). Final state bremsstrahlung photons were generated for the electron and muon modes according to an approximate distribution.³⁸

The momentum and direction of each track were then adjusted to account for the resolution of CELLO detector. The tracking efficiency and the particle identification efficiencies of the CELLO detector were simulated according to parameterizations that are given in Ref. 35. The selection criteria that were used in Ref. 35 were then applied to the simulated events. The two most significant of these criteria were that no photons³⁹ of energy larger than 5% of the beam energy were allowed in the region of polar angle $|\cos\theta| < 0.99$, and that only three particles were required to be identified.

The analysis was performed as follows: first, a hypothesis was made for the branching ratios of the doubly-charged Higgs boson. Next, a Higgs mass

was selected. The Monte Carlo simulation was then used to calculate the number of events in each of the three categories ($eeee$, $ee\mu\mu$, and $\mu\mu\mu\mu$) that would be expected for each beam energy and luminosity. The total number of events in each category was then adjusted to account for the vertex and trigger efficiencies that are reported in Ref. 35. The assumed Higgs mass was then incremented and the procedure was repeated several times. Finally, the information listed in Table II was used in a standard Poisson statistical analysis⁴⁰ to extract a 90% confidence limit on M_Δ for the given branching ratio hypothesis.

Four branching ratio hypotheses were considered. They are listed in Table III along with the corresponding limits on M_Δ . Note that there was sufficient leakage of the tau decay modes into the electron and muon channels that it was possible to find a moderate mass limit in the case that 100% of the Higgs bosons decay into tau final states. This limit is shown as a horizontal line in Fig. 2. Technically, the coupling constant $g_{\tau\tau}$ is displayed along horizontal axis in this case. However, since we have implicitly assumed that $g_{ee}^2, g_{\mu\mu}^2 \ll g_{\tau\tau}^2$, the limit applies to all three coupling constants.

5. CONCLUSIONS

We have considered the effect of a doubly-charged Higgs boson on several processes. We find that the existence of such objects is excluded at a 90% confidence level for Higgs masses less than 14 GeV. If the coupling constant g_{ee} is larger than approximately 0.075, the limit becomes more stringent. For a Higgs boson that is strongly coupled to electrons ($g_{ee} = \sqrt{4\pi}$), the limit increases to 1.25 TeV. If the coupling of the Higgs boson to the charged leptons is non-diagonal in lepton flavor, a much more stringent limit applies.

We note that more sensitive searches for doubly-charged Higgs bosons can be performed at the current generation of hadron colliders and Z^0 factories. The coupling of the Z^0 to the left-handed Higgs boson is quite large (the coupling of the Z^0 to the right-handed Higgs is much smaller). The signature of an event is sufficiently spectacular that it can be identified quite easily, even in the difficult environment of a hadron collider.

ACKNOWLEDGMENTS

The work presented in this document has benefited greatly from several discussions with Michael Peskin. His careful scrutiny of an earlier version of this article prevented the dissemination of a major blunder which, although traceable to a mistake in a popular textbook, should have been noted by the author. The author also wishes to thank Ken Moffeit for his careful reading of this document. His comments have helped to make the prose a bit less obscure. Finally, the author would like to thank B.F.L. Ward for helping to clarify a misleading article and Isard Dunietz for pointing out some very useful literature on B meson mixing.

REFERENCES

1. We use the verb *to know* from a comfortable, historical point of view.
2. A change of lepton flavor ΔL_f is defined as the change in lepton number for *each* species of lepton.
3. C. N. Yang and J. Tiomno, *Phys. Rev.* **79**, 495 (1950);
G. Feinberg and S. Weinberg, *Nuovo Cimento* **14**, 5711 (1959);
G. Feinberg, P. K. Kabir, and S. Weinberg, *Phys. Rev. Lett.* **3**, 527 (1959);
N. Cabibbo and R. Gatto, *Phys. Rev. Lett.* **5**, 114 (1960);
E. Derman, *Phys. Lett.* **78B**, 497 (1978).
4. G. Feinberg and S. Weinberg, *Phys. Rev. Lett.* **6**, 381 (1961);
G. Feinberg and S. Weinberg, *Phys. Rev.* **123**, 1439 (1961).
5. J. J. Amato *et al.*, *Phys. Rev. Lett.* **21**, 1709, 1786(E) (1968).
6. All limits given will be single-sided 90% confidence limits unless otherwise stated.
7. W. C. Barber, B. Gittelman, D. C. Cheng, and G. K. O'Neill, *Phys. Rev. Lett.* **22**, 902 (1969).
8. G. M. Marshall, J. B. Warren, C. J. Oram, and R. F. Kiefl, *Phys. Rev.* **D25**, 1174 (1982);
G. A. Beer *et al.*, *Phys. Rev. Lett.* **57**, 671 (1986); B. Ni *et al.*, *Phys. Rev. Lett.* **59**, 2716 (1987).
9. T. M. Huber *et al.*, TRI-PP-88-30, May 1988;
T. M. Huber *et al.*, TRI-PP-88-53, June 1988.
10. S. E. Willis *et al.*, *Phys. Rev. Lett.* **44**, 522, 370(E) (1980).
11. F. Bergsma *et al.*, *Phys. Lett.* **122B**, 465 (1983).

12. Note that all diagrams can be reordered to describe the process $e^-e^- \rightarrow \mu^-\mu^-$.
13. J. S. Hagelin, *Nucl. Phys.* **B193**, 123 (1981);
A. J. Buras, W. Slominski, and H. Steger, *Nucl. Phys.* **B245**, 369 (1984).
14. A. Halprin, *Phys. Rev. Lett.* **48**, 1313 (1982).
15. K. Ishikawa, S. Midorikawa, T. Moriya, and M. Yoshimura, *Prog. in Theor. Phys.* **57**, 2158 (1977).
16. T. G. Rizzo, *Phys. Rev.* **D25**, 1355 (1982).
17. G. K. Leontaris, K. Tamvakis, and J. D. Vergados, *Phys. Lett.* **162B**, 153.
18. E. G. Drukarev, V. A. Gordeev, and A. I. Mikhailov, Leningrad-87-1317, August 1987.
19. G. B. Gelmini and M. Roncadelli, *Phys. Lett.* **99B**, 411 (1981);
R. N. Mohapatra and J. D. Vergados, *Phys. Rev. Lett.* **47**, 1713 (1981);
H. Georgi and M. Machacek, *Nucl. Phys.* **B262**, 463 (1985).
20. A good review of right-left symmetric models is R. N. Mohapatra, *Proc. of the NATO Advanced Study Inst.: Quarks, Leptons, and Beyond*, ed. H. Fritzsch *et al.*, Plenum Publishing Co. (New York, 1985), pg. 219.
21. In right-left symmetric models, the Δ_R and Δ_L triplets are not involved in the generation of the masses of the charged leptons. Their couplings to the light leptons are therefore not suppressed. The coupling of the right-handed Higgs boson to the charged leptons may in fact be much larger than that of its left-handed counterpart (because it is necessary to break the right-left symmetry and give the right-handed W boson a large mass).

22. The measurements of the K_l-K_s mass difference and the anomalous magnetic moments of the electron and muon have, for example, placed rather tight constraints on many hypothetical processes. A recent study of the process $e^+e^- \rightarrow \mu^+\mu^-$ has yielded new limits on neutral current lepton number violation. See K. K. Gan, *Phys. Lett.* **209B**, 95 (1988).
23. E. J. Eichten, K. D. Lane, and M. E. Peskin, *Phys. Rev. Lett.* **50**, 811 (1983).
24. TASSO Collaboration: M. Althoff *et al.*, *Z. Phys.* **C22**, 13 (1984);
W. Braunschweig *et al.*, *Z. Phys.* **C37**, 171 (1988).
25. PLUTO Collaboration: C. Berger *et al.*, *Z. Phys.* **C27**, 341 (1985).
26. HRS Collaboration: M. Derrick *et al.*, *Phys. Lett.* **166B**, 463 (1986);
M. Derrick *et al.*, *Phys. Rev.* **D34**, 3286 (1986).
27. MAC Collaboration: E. Fernandez *et al.*, *Phys. Rev.* **D35**, 10 (1987).
28. F. A. Berends and R. Kleiss, *Nucl. Phys.* **B206**, 61 (1983);
F. A. Berends and R. Kleiss, *Nucl. Phys.* **B228**, 537 (1983).
29. For the weak neutral current, this is confirmed in M. Böhm, A. Denner, and W. Hollik, *Nucl. Phys.* **B304**, 687 (1988).
30. U. Amaldi *et al.*, *Phys. Rev.* **D36**, 1385 (1987).
31. See for example: R. Engfer and H. K. Walter, *Annu. Rev. Nucl. Part. Sci.* **36**, 327 (1986);
R. E. Shrock, ITP-SB-88-28, May 1988.
32. U. Bellgardt *et al.*, *Nucl. Phys.* **B299**, 1 (1988).
33. CELLO Collaboration: H. J. Behrend *et al.*, DESY 84-103, October 1984.
34. JADE Collaboration: W. Bartel *et al.*, *Z. Phys.* **C30**, 545 (1986).

35. F. Le Diberder, Thèse d'Etat, Université de Paris-Sud, Centre d'Orsay, LAL 88-21, June 1988.
36. F. A. Berends, P. H. Daverveldt, and R. Kleiss, *Nucl. Phys.* **B253**, 441 (1985).
37. O. Nicosini and L. Trentadue, *Phys. Lett.* **B185**, 395 (1987).
38. We use a form that is appropriate for the decay $Z^0 \rightarrow \ell\ell\gamma$. See M. Caffo, R. Gatto, and E. Remiddi, *Phys. Lett.* **139B**, 439 (1984);
F. A. Berends and R. Kleiss, *Z. Phys.* **C27**, 365 (1985).
39. Any photon-charged track pair that are less than 10° apart in space angle and form an invariant mass that is less than 10% of the beam energy are merged.
40. The Particle Data Group, *Phys. Lett.* **170B** (1986).

Table I

A summary of several measurements of the cross section for Bhabha Scattering.

Experiment	\sqrt{s} (GeV)	$\int Ldt$ (pb)	# of Events	Angular Region
PLUTO ²⁵	34.8	41.8	59,238	$-0.8 \leq \cos \theta \leq 0.8$
TASSO ²⁴	34.8	174.5	166,348	$-0.8 \leq \cos \theta \leq 0.8$
HRS ²⁶	29.0	164.8	84,423	$-0.55 \leq \cos \theta \leq 0.55$
MAC ²⁷	29.0	127.6	584,267	$0.0 \leq \cos \theta \leq 0.9$

Table II

The number of four lepton events that were observed in the data of the CELLO Collaboration.³⁵ The theoretical expectation is based upon a modified version of a Monte Carlo program by Berends, Daverveldt, and Kleiss.³⁶

Final State	Number of Events	Theoretical Expectation
$eeee$	16	15
$ee\mu\mu$	8	10
$\mu\mu\mu\mu$	1	0.7

Table III

The 90% confidence limit on M_Δ for several branching ratio hypotheses.

$\text{Br}(\Delta \rightarrow ee)$	$\text{Br}(\Delta \rightarrow \mu\mu)$	$\text{Br}(\Delta \rightarrow \tau\tau)$	Limit on M_Δ (GeV)
1.00	0.00	0.00	21.5
0.00	1.00	0.00	21.8
0.00	0.00	1.00	14.0
0.33	0.33	0.33	20.9

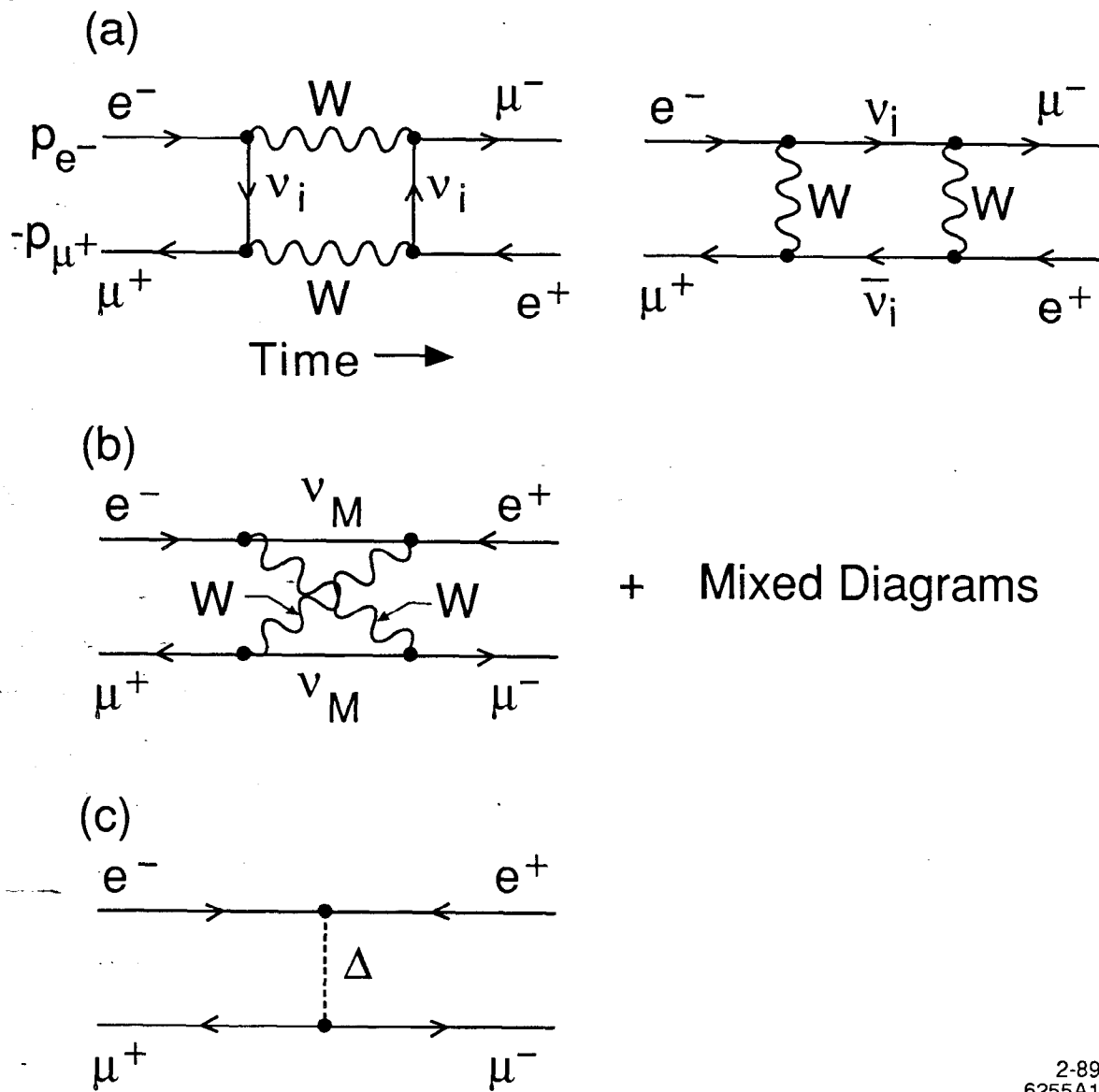
FIGURE CAPTIONS

Fig. 1. Three possible subprocesses for muonium to antimuonium conversion. Diagram (a) represents a second-order exchange of ordinary Dirac neutrinos. Diagram (b) is a similar process but with Majorana neutrinos instead. Diagram (c) represents the t-channel exchange of a doubly-charged Higgs boson. Note that all diagrams can be reordered to describe the process $e^-e^- \rightarrow \mu^-\mu^-$.

Fig. 2. The 90% confidence contours of M_Δ versus $\sqrt{g_{ee}g_{\mu\mu}}$ and g_{ee} that are obtained from several processes. The limit that is obtained from the published limit on muonium to antimuonium conversion⁹ is shown as a dotted line ($\sqrt{g_{ee}g_{\mu\mu}}$ is plotted along the horizontal axis). The limit that is obtained from the Bhabha scattering data of several PEP and PETRA experiments²⁴⁻²⁷ is shown as a solid curve (g_{ee} is plotted along the horizontal axis). The coupling-independent limit that is obtained from a measurement of four-lepton production³⁵ is shown as the horizontal dashed-dotted line. For reference, the sizes of the coupling constants g , g' , and e are indicated. The strong coupling limit occurs at the value $\sqrt{4\pi}$.

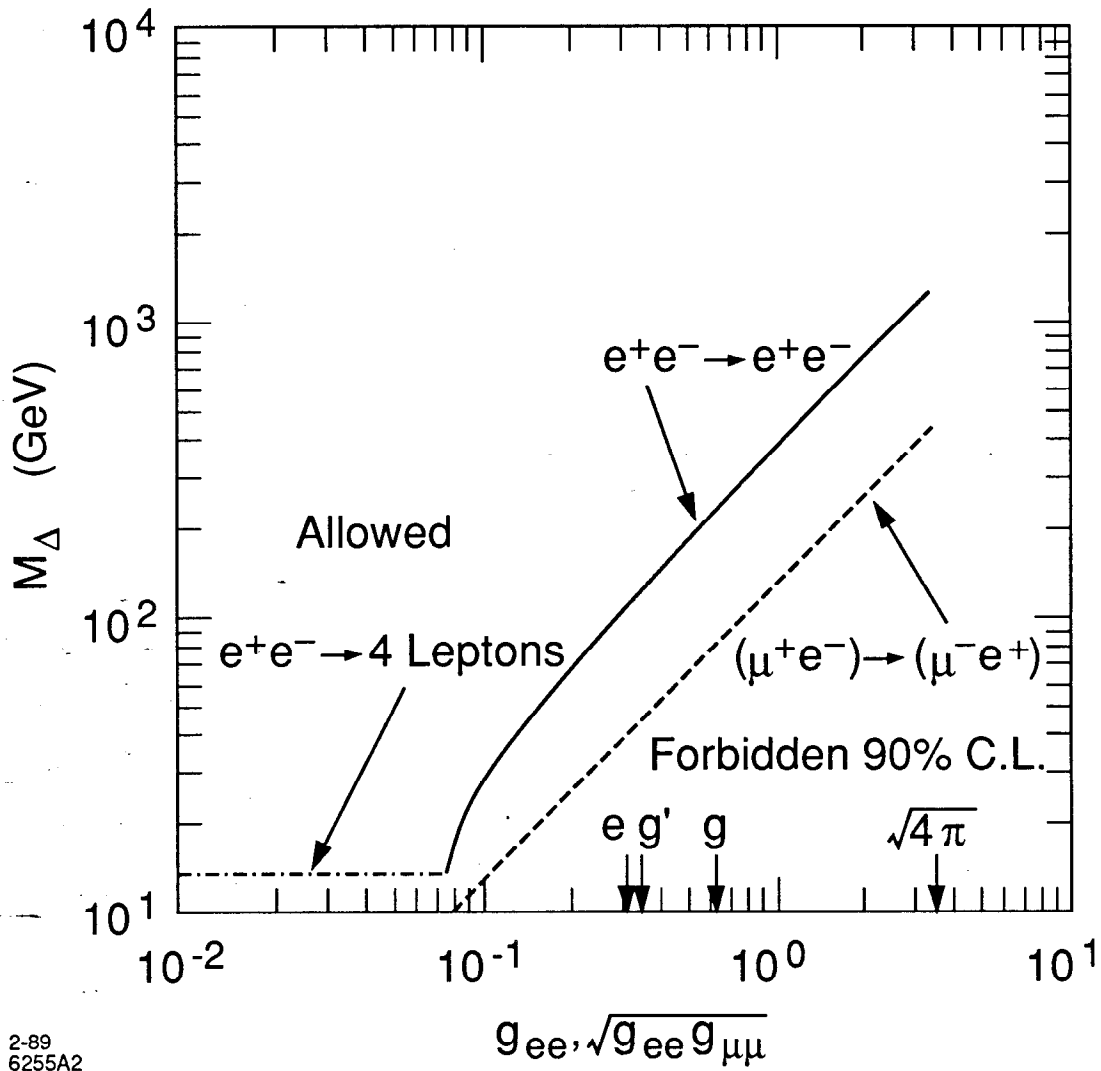
Fig. 3. The contribution of a doubly-charged Higgs scalar to Bhabha scattering.

Fig. 4. The decay $\mu^- \rightarrow e^-e^+e^-$ as mediated by a Δ^{--} .



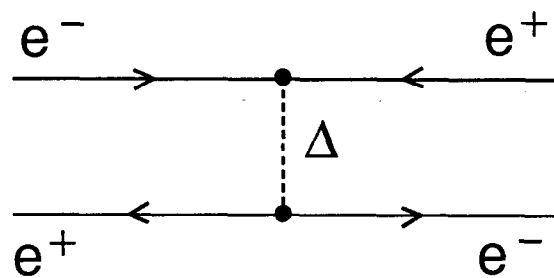
2-89
6255A1

Fig. 1



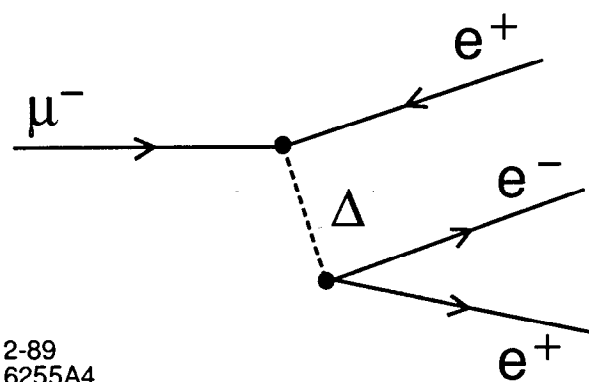
2-89
6255A2

Fig. 2



2-89
6255A3

Fig. 3



2-89
6255A4

Fig. 4